Appl. Phys. B 53, 308–313 (1991)

Applied Physics B Photophysics and Laser Chemistry

Two-Photon Absorption-Induced Thermal Effects in Platinum Poly-ynes

S. Guha, K. Kang, and P. L. Porter

Martin Marietta Laboratories, 1450 South Rolling Road, Baltimore, MD 21227, USA

Received 17 May 1991/Accepted 13 September 1991

Abstract. We present here a theoretical study of the nonlinear effect arising from one- and two-photon absorption-induced self defocusing in liquids. Experimental results demonstrate power limiting of 10 ns, 532 nm laser pulses by linear and two-photon absorption in concentrated solutions of platinum poly-ynes.

PACS: 42.65

The large electron delocalizations in the molecular structures of organic compounds and polymers are commonly exploited to obtain materials with large third-order optical nonlinearities. In our previous work [1, 2] we showed that platinum poly-ynes constitute a class of organometallic polymers with high values of nonlinearity, as well as broadband transparency in the visible and the near IR. Using picosecond Nd : YAG laser pulses, we determined that two-photon absorption is the dominant nonlinearity for wavelengths in the 500 to 750 nm range – the imaginary part of the third order susceptibility, χ^3, which gives rise to two-photon absorption, is generally larger than the real part of χ^3 by an order of magnitude or more in the visible wavelengths. Thus, nonlinear absorption is expected to be much stronger than nonlinear refraction. However, our power-limiting measurements with nanosecond laser pulses on concentrated solutions of the platinum poly-ynes also indicated nonlinear refraction of the laser beam, which we attribute to the thermal lensing effect created by both the linear and the nonlinear absorption of the laser beam in the solution.

In the work reported here, we develop a theoretical description of this complicated nonlinear response. This nonlinearity cannot simply be characterized by a refractive index change $n_2 I$ proportional to the laser intensity I because the order of the effective susceptibility is higher than 3. The effect is similar to that in semiconductors such as GaAs, ZnSe, or HgCdTe, in which the dominant bound electronic nonlinearity is absorptive, but the linear and nonlinear absorption-induced free carriers cause large refractive nonlinear effects as well [3]. We start our theoretical discussion with a series of equations which describe the phase change of a laser beam arising from the linear and the nonlinear absorption-induced thermal-lensing effects. We then determine the effect of this phase change on the subsequent free-space propagation of the laser beam by calculating the near field, on-axis, laser beam intensity transmitted through the polymer solution as a function of the incident energy. Finally, these theoretical results are compared with experimental observations on a platinum poly-yne solution.

1 Theory

1.1 Nonlinear Changes in Intensity and Phase

The intensity (I) of a laser beam propagating in the z direction through a thin nonlinear medium with linear absorption coefficient α and two-photon absorption coefficient β is given by the equation

$$\frac{dI}{dz} = -\alpha I - \beta I^2 . \tag{1}$$

If the spatial and temporal profile of the incident laser beam is nonuniform – say, Gaussian – its absorption causes nonuniform heating of the medium. The result is a nonuniform change in the temperature distribution (ΔT), which in turn, gives rise to a nonuniform change in the refractive index (Δn):

$$\Delta n = \frac{dn}{dT} \Delta T , \tag{2}$$

where dn/dT denotes the temperature gradient of the refractive index of the medium. The phase change ($\Delta\phi$) arising from this Δn is given by the equation:

$$\frac{d(\Delta\phi)}{dz} = \frac{2\pi}{\lambda} \frac{dn}{dT} \Delta T . \tag{3}$$

The temperature change ΔT due to heating by the cylindrically symmetric laser beam is obtained from the heat diffusion equation:

$$c\varrho \frac{d\Delta T}{dt} = Q + k\nabla^2(\Delta T), \tag{4}$$

where c denotes the specific heat of the medium, ϱ is its density, and Q is the amount of heat generated per unit length per unit time by the absorbed laser beam, given by

$$Q = \frac{1}{J}\frac{dI}{dz}. \tag{5}$$

The solution to (4) gives the temperature distribution at a point with cylindrical coordinates (r_1, z) at a time t for the distributed source Q in terms of the Green's function $G(r_1, r_1', t)$ [4]:

$$\Delta T(r_1, z, t) = \int_{-\infty}^{t} dt' \int_{0}^{\infty} dr_1' 2\pi r_1' Q(r_1', t', z) G(r_1, r_1', t'). \tag{6}$$

The expression for the appropriate Green's function in this case is given by Carslaw and Jaeger [5]:

$$G(r_1, r_1', t') = \frac{1}{4\pi k t'} \exp\left[\frac{-(r_1^2 + r_1'^2)}{4\kappa t'}\right] I_0\left(\frac{r_1 r_1'}{2\kappa t'}\right), \tag{7}$$

where k is the termal conductivity of the medium and κ is the thermal diffusivity.

If l denotes the thickness of the medium, then the phase change $\Delta\phi$ at the beam exit of the medium is obtained from (3), (5), and (6):

$$\Delta\phi(r_1, l, t) = \frac{4\pi^2}{\lambda J}\frac{dn}{dT}\int_{-\infty}^{t} dt' \int_{0}^{\infty} dr_1' r_1' G(r_1, r_1', t') \times [I(r_1', t', l) - I(r_1', t', 0)]. \tag{8}$$

The intensity $I(r, t, z)$ is easily obtained from (1):

$$I(r, t, z) = \frac{I(r, t, 0)\exp(-\alpha z)}{1 + \beta I(r, t, 0) z A_z}, \tag{9}$$

where $A_z = [(1 - \exp(-\alpha z)]/(\alpha z)$. If we assume the laser beam to be focused at the entrance plane of the nonlinear medium (i.e., at $z = 0$), we can write the incident intensity in terms of the peak intensity I_p:

$$I(r, t, 0) = I_p \exp\left(-\frac{r^2}{r_0^2} - \frac{t^2}{\tau^2}\right). \tag{10}$$

Then, by defining the dimensionless parameters

$$r_{11} = r_1/r_0, \quad r_{11}' = r_1'/r_0,$$
$$t_1 = t/\tau, \quad t_1' = t'/\tau, \quad l_1 = l/z_0,$$

where $z_0 = 2\pi r_0^2/\lambda$, and substituting (7), (9), and (10) in (8), we can express the phase change $\Delta\phi$ as

$$\Delta\phi(r_{11}, l_1, t_1) = \Delta\phi_0 \int_{-\infty}^{t_1} dt_1' \int_{0}^{\infty} dr_1' F(r_{11}, r_{11}', t_1'). \tag{11}$$

Here

$$\Delta\phi_0 = \frac{\pi A_l (dn/dT) I_p r_0^2}{\lambda k J} \tag{12}$$

and

$$F(r_{11}, r_{11}', t_1') = \frac{\exp\left[-\dfrac{p_1(r_{11}^2 + r_{11}'^2}{2t_1'}\right]}{t_1'} I_0\left(\frac{p_1 r_{11} r_{11}'}{t_1'}\right) \times f_1 \frac{\alpha l + b_1 f_1}{1 + A_l b_1 f_1}, \tag{13}$$

where

$$p_1 = r_0^2/(2\kappa\tau), \quad A_l = [1 - \exp(-\alpha l)]/\alpha l,$$
$$b_1 = \beta I_p l = \frac{\beta E_0 l}{\pi\sqrt{\pi} r_0^2 \tau}, \quad f_1 = \exp[-(r_1'^2 + t_1'^2)],$$

and E_0 denotes the total amount of incident laser energy. As shown below, we use I_p, αl, and βl as parameters to determine the dependence of the nonlinear phase change $\Delta\phi$, and later the transmitted beam intensity, on the incident energy and the linear and nonlinear absorption.

1.2 Beam Propagation Equations

The nonlinearity in the phase of the laser beam due to its propagation through the nonlinear medium can be evaluated from the dependence of various beam parameters (such as the on-axis intensity measured at a nearfield position) on the incident intensity. To determine theoretically the intensity of a beam transmitted through a nonliner medium and then propagated through free space, we used the usual Fresnel approximation and the hypothetical optical arrangement shown in Fig. 1, where z denotes the distance between the exit plane of the nonlinear medium and the plane of a detector.

Denoting the radial coordinate at this plane by r_2, and using the dimensionless notation

$$r_{21} = r_2/r_0, \quad z_{11} = (z + l)/z_0.$$

we can write the electric field $E(r_{21}, z_{11}, t_1)$ at the detector plane in terms of the field $E(r_{11}, l_1, t_1)$ at the exit plane [6]:

$$E(r_{21}, z_{11}, t_1) = \frac{\exp(i\pi r_{21}^2/2z_{11})}{iz_{11}} \int_{0}^{\infty} E(r_{11}, l_1, t_1) \times \exp(ir_{11}^2/2z_{11}) J_0(r_{11} r_{21}/z_{11}) r_{11} dr_{11}. \tag{14}$$

The field at the exit plane is expressed in terms of the beam intensity and the phase:

$$E(r_{11}, l_1, t_1) \equiv \sqrt{2I(r_{11}, l_1, t_1)/c\varepsilon_0}\, e^{i\phi(r_{11}, l_1, t_1)}. \tag{15}$$

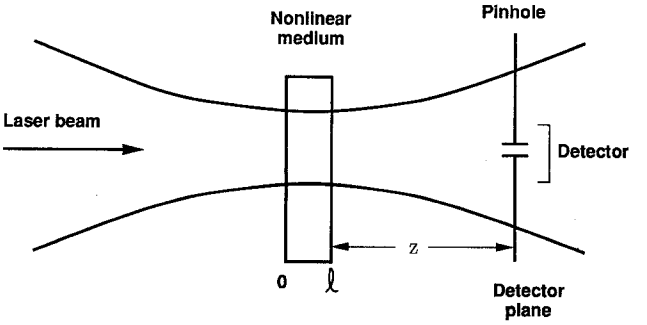

Fig. 1. A schematic of the optical arrangement assumed for the theoretical study

If the phase change arising from the nonlinearity of the sample is denoted by $\Delta\phi$,

$$\phi(r_{11}, l_1, t_1) = \phi(r_{11}, 0, t_1) + \Delta\phi + \text{constant}. \tag{16}$$

Inserting (9) and (11) into (15) and (16) then gives the intensity distribution at the detector plane, which can be written in terms of the peak incident intensity I_p:

$$I(r_{21}, z_{11}, t_1) = I_p \exp(-\alpha l)\,|S|^2, \tag{17}$$

where

$$S = \int_0^\infty \frac{\exp\left(-\frac{r_{11}^2}{2} - \frac{t_1^2}{2}\right)}{\sqrt{1+b_1 f_1}} \exp\left[i\left(\frac{r_{11}^2}{2z_{11}} + \Delta\phi\right)\right] \times J_0\left(\frac{r_{11} r_{21}}{z_{11}}\right) r_{11} dr_{11}. \tag{18}$$

The integrals in (11) and (18) are evaluated numerically, as discussed below.

2 Results

2.1 The Phase Change $\Delta\phi$

In calculating the amount of phase change $\Delta\phi$ for usual experimental conditions from (11), we can make a few simplifying approximations that reduce the number of numerical integrations. For the usual liquid solvents, we can assume a value for κ of about $10^{-3}\,\text{cm}^2/\text{s}$; then the parameter p_1 for a 10 ns laser pulse (i.e., for $\tau = 10^{-8}$ s) is equal to $500 r_0^2$, where r_0 is expressed in microns. For visible laser wavelengths, r_0 is usually 1 or higher, which makes p_1 more than 500. Because the temporal pulse shape is assumed to be Gaussian, the maximum value of t_1' in (13) can be taken as about 10, making the parameter $p_1/2t_1'$ always bigger than 25. For the experimental case described in the next section, r_0 is about 100 μm, so that $p_1/2t_1'$ is more than 25×10^4. If we rewrite (13) as

$$F(r_{11}, r_{11}', t_1') = B_1 \exp\left(-\frac{p_1 r_{11} r_{11}'}{t_1'}\right) I_0\left(\frac{p_1 r_{11} r_{11}'}{t_1'}\right) \times f_1 \frac{\alpha l + b_1 f_1}{1 + A_l b_1 f_1}, \tag{19}$$

where

$$B_1 = \frac{\exp\left[-\frac{p_1}{2t_1'}(r_{11} - r_{11}')^2\right]}{t_1'} \tag{20}$$

then, for large $p_1/2t_1'$, B_1 can be replaced by

$$\sqrt{\frac{2\pi t_1'}{p_1}}\,\delta(r_{11} - r_{11}'). \tag{21}$$

When $r_{11} \neq 0$, the delta function can be inserted in (13) and the r' integration in (11) is easily performed to give

$$\Delta\phi(r_{11}, l_1, t_1) = \Delta\phi_0 \sqrt{\frac{2\pi}{p_1}} \int_{-\infty}^{t_1} \frac{dt_1'}{\sqrt{t_1'}} r_{11}\, e^{-\frac{p_1 r_{11}^2}{t_1'}} \times I_0\left(\frac{p_1 r_{11}^2}{t_1'}\right) f_{11} \frac{\alpha l + b_1 f_{11}}{1 + A_l b_1 f_{11}}. \tag{22}$$

Here, $f_{11} = \exp[-(r_{11}^2 + t_1'^2)]$. Using (9.8.2) in [7], we can finally write the expression for the phase change as

$$\Delta\phi = \Delta\phi_{00} \int_{-\infty}^{t_1} dt_1' f_0\left(\frac{p_1 r_{11}^2}{t_1'}\right) f_{11} \frac{\alpha l + b_1 f_{11}}{1 + A_l b_1 f_{11}}. \tag{23}$$

Here

$$\Delta\phi_{00} = \frac{\sqrt{2\pi}\Delta\phi_0}{p_1} = \frac{2\pi\sqrt{2\pi}\kappa\tau A_l (dn/dT) I_p}{\lambda J k}$$

and

$$f_0(y) = 0.39894228 + 0.0498222/y + 0.031685484/y^2 - 0.083090918/y^3 + 1.811981469/y^4 - 15.25947748/y^5 + 73.29202549/y^6 - 171.8222318/y^7 + 153.4453331/y^8.$$

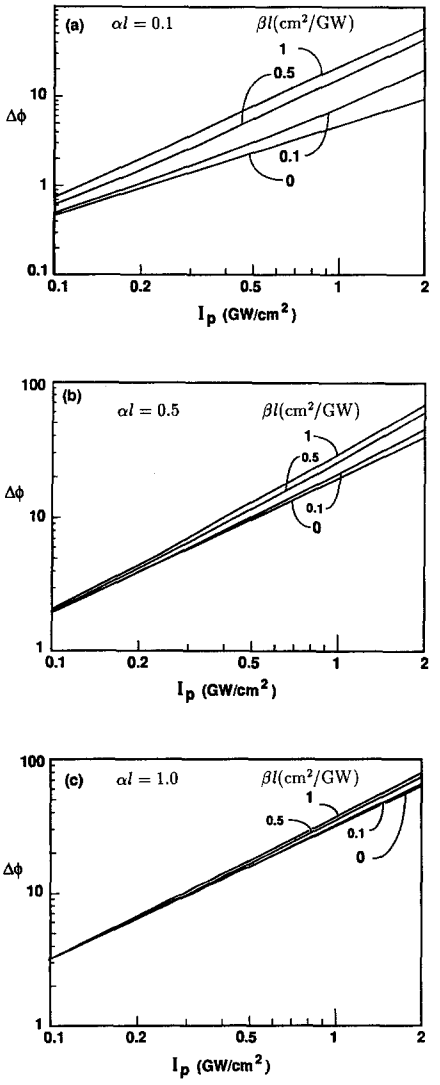

Fig. 2a–c. Beam phase change ($\Delta\phi$) vs peak beam intensity (I_p) for different values of linear absorption (αl) and two-photon absorption (βl). **a** $\alpha l = 0.1$, $\beta l = 0$, 0.1, 0.5, 1.0 cm²/GW; **b** $\alpha l = 0.5$, $\beta l = 0$, 0.1, 0.5, 1.0 cm²/GW; **c** $\alpha l = 1.0$, $\beta l = 0$, 0.1, 0.5, 1.0 cm²/GW

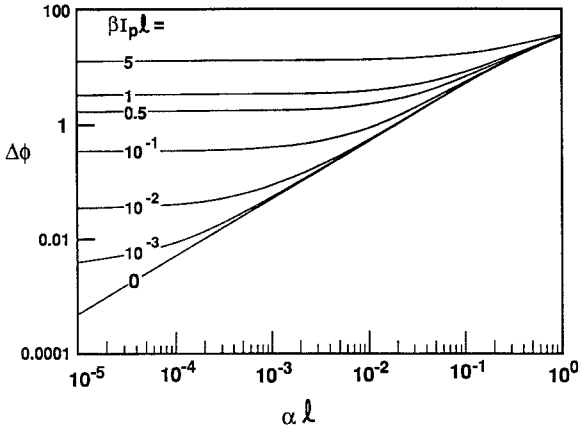

Fig. 3. Beam phase change ($\Delta\phi$) vs linear absorption (αl) for different values of $\beta I_p l$

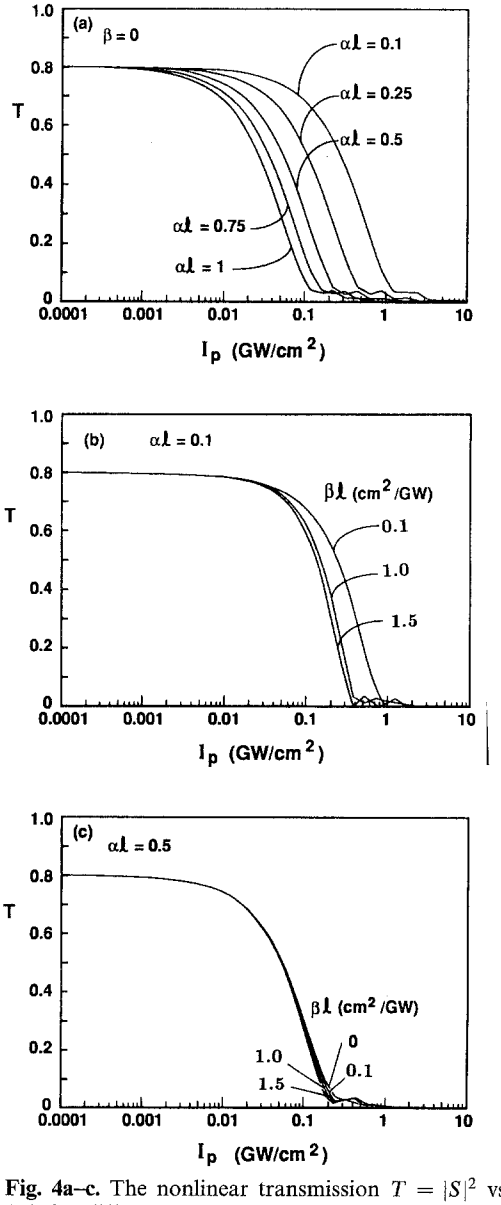

Fig. 4a–c. The nonlinear transmission $T = |S|^2$ vs peak intensity (I_p) for different values of linear absorption (αl) and two-photon absorption (βl). **a** $\beta l = 0$, $\alpha l = 0.1, 0.25, 0.5, 0.75, 1.0$; **b** $\alpha l = 0.1$, $\beta l = 0.1, 1.0, 1.5\,\mathrm{cm^2/GW}$; **c** $\alpha l = 0.5$, $\beta l = 0.1, 1.0, 1.5\,\mathrm{cm^2/GW}$

For $r_{11} = 0$

$$\Delta\phi = \frac{\Delta\phi_{00}}{\sqrt{2\pi}} \int_{-\infty}^{t_1} e^{-t_1'^2} \frac{\alpha l + b_1 e^{-t_1'^2}}{1 + A_l b_1 e^{-t_1'^2}} dt_1' . \tag{24}$$

2.2 $\Delta\phi$ vs I_p for Different Values of αl and βl

With $\kappa = 10^{-3}\,\mathrm{cm^2/s}$, $\tau = 10^{-8}\,\mathrm{ns}$, $dn/dT = 10^{-4}\,\mathrm{K^{-1}}$, $\lambda = 0.532 \times 10^{-4}\,\mathrm{cm}$, $J = 4.2\,\mathrm{J/cal}$, and $k = 10^{-3}\,\mathrm{cal/K/s/cm}$, $\Delta\phi_{00} = 28 A_l I_p$, where I_p is expressed in $\mathrm{GW/cm^2}$. Figure 2 shows a plot of $\Delta\phi$ at $r_{11} = 0$ as a function of I_p for different values of αl and βl. For $\beta l = 0$, the slope of the curve in log–log scale is 1, showing that the nonlinearity in this case is of the "n_2 type." For $\beta l \neq 0$, not only is the slope of the log–log plot for small I_p larger than 1, but the curve is not linear for higher values of I_p. In other words, the order of the effective nonlinearity is higher than 3 for low intensities, and the nonlinearity does not obey a power law at higher intensities. We also note from Fig. 2 that the contribution of the nonlinear absorption to the phase change is substantial only at small values of linear absorption.

Figure 3 shows that the peak (i.e., at the time $t_1 = 0$) on-axis phase change values for even widely different $\beta I_p l$ are close to each other for $\alpha l > 0.4$.

2.3 Transmitted Intensity as a Function of I_p, αl and βl

The nonlinear phase change imparted to the laser beam by its passage through the medium is manifested by a nonlinear change in the beam intensity measured outside the medium. We consider here the transmitted intensity measured at a distance $z_{11} = 0.5$. Figure 4 displays plots of the value of the quantity $|S|^2$ obtained from (18) vs peak intensity; the phase change $\Delta\phi$ was calculated from (11). As expected, the nonlinear absorption lowers the value of the incident intensity at which the transmission starts to drop. For small linear absorption ($\alpha l = 0.1$), the presence of the nonlinear absorption βl causes a large change in the transmitted intensity; for larger αl, the effect of βl is not appreciable. This result is summarized in Fig. 5, where $T_{1/2}$, the value of I_p at which $|S|^2$ drops to half of its value at low intensity, is plotted as a function of αl for different values of βl. For $\alpha l > 0.4$, $T_{1/2}$ becomes independent of βl and depends only on the value of αl.

The theoretical plots in Fig. 6 correspond to experimental curves presented later. Here, the transmission T is plotted as a function of the incident intensity I_p for $\alpha l = 0.2$; $\beta l = 0$ for Fig. 6a and $\beta l = 2\,\mathrm{cm^2/GW}$ for Fig. 6b and c. However, for Fig. 6b the contribution of the nonlinear absorption to $\Delta\phi$ is zero. The drop in transmission for this plot arises from self defocusing due to linear absorption, and from the reduction of the transmitted beam energy due to nonlinear absorption. The close match between the curves of Figs. 6a and 6b and the large disparity between those of Fig. 6b and c show that the effect of the nonlinear absorption-induced thermal defocusing is very significant and cannot be ignored.

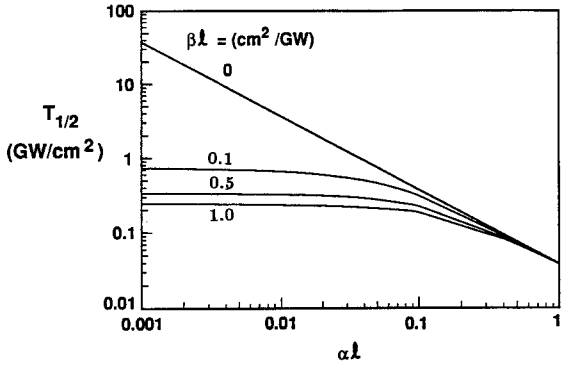

Fig. 5. $T_{1/2}$ (the value of I_p in GW/cm^2 at which nonlinear transmission falls to 1/2 its value at low intensity vs liner absorption (αl) for two-photon absorption (βl) = 0, 0.1 0.5, 1.0 cm^2/GW

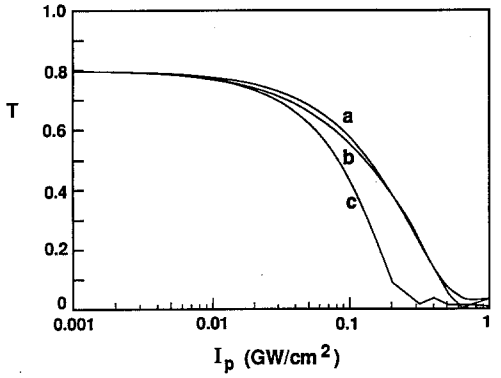

Fig. 6. The nonlinear transmission $T = |S|^2$ vs peak intensity (I_p) for linear absorption ($\alpha l = 0.2$). *a* two-photon absorption (βl) = 0; *b* and *c* $\beta l = 2\,\mathrm{cm}^2/\mathrm{GW}$. In *b* the contribution of the nonlinear absorption to the phase change is ignored

3 Experimental Results

To verify our theoretical results, we performed experiments using a power-limiting configuration similar to that shown schematically in Fig. 1 and a 10 ns, 532 nm wavelength doubled Nd:YAG laser beam focused to a spot size of 100 μm (HWe^{-1}M). The nonlinear medium was a solution of platinum poly-yne or iodine in tetrahydrofuran (THF) in 2 mm-pathlength cells. The concentrations of the two solutions were adjusted to equalize their linear absorptions (for both solutions αl was 0.2). The iodine solution exhibited no nonlinear absorption, and the platinum polymer solution showed both linear and nonlinear absorption. The transmitted intensity was monitored by a detector at a normalized distance $z_{11} = 0.5$, both with and without a small pinhole placed in front of it. Without the pinhole, the area of the detector was large enough to intercept the entire transmitted beam at both high- and at low-incident intensities.

Nonlinear absorption was manifested by a nonlinear dependence of the transmitted intensity in the absence of the pinhole. As seen in Fig. 7a, the transmission of the iodine solution with no pinhole present is independent of the incident intensity – i.e., there is no nonlinear absorption. With the pinhole in front of the detector, the transmission of the iodine solution drops (Fig. 7b), demonstrating the effect of thermal defocusing.

The transmission of the platinum poly-yne solution in the absence of the pinhole (Fig. 7c) indicates the presence of nonlinear absorption, specifically two-photon absorption. Because the absorption coefficients of the iodine and the polymer solutions were chosen to be the same, the difference in transmission between Fig. 7b and c corresponds to the difference between Fig. 6a and b. As was expected from our theoretical analysis, the transmission difference between Fig. 7b and c is small. With the pinhole in front of the detector (Fig. 7d), the transmitted intensity drop is much more significant, as was expected from the theoretical behavior shown in Fig. 6c. This decrease in transmission is thus most likely due to the nonlinear absorption-induced thermal lensing. The change in the transmitted intensity at a given incident intensity, both with and without the pinhole, qualitatively confirms that the nonlinear absorption leads to an increased amount of defocusing in the transmitted beam; more quantiative proof of this effect will be reported in future.

4 Summary

Both linear and two-photon absorption in a liquid cause a nonlinear change in the phase of a laser beam prop-

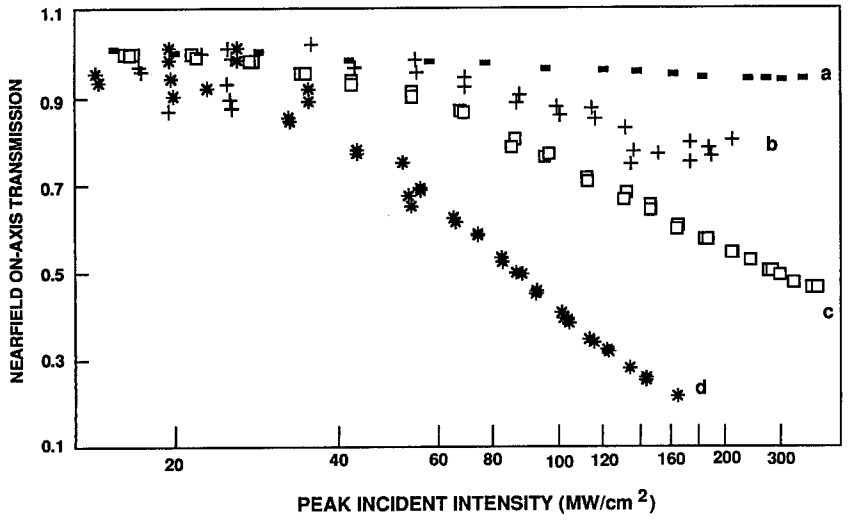

Fig. 7. Experimentally obtained near field nonlinear transmissions vs incident peak intensity: *a* iodine solution, with no pinhole before detector. *b* Iodine solution with pinhole before the detector; *c* platinum poly-yne solution with no pinhole before the detector, *d* Poly-yne solution with a pinhole before the detector

agating through it. In addition, two-photon absorption changes the intensity of the transmitted laser beam. We determined the intensity dependence of the on-axis phase change of a transmitted beam for different values of linear and nonlinear absorption coefficients. We also evaluated the value of the transmitted on-axis intensity at a nearfield point as a function of the incident intensity.

Our results show that two-photon absorption effects cause substantial changes in the transmitted intensity only for low values of the linear absorption. This finding has implications for the use of the nonlinear absorption effect in the fabrication of nonlinear devices, such as optical switches or power limiters. A partial experimental confirmation of the theory is also presented here.

References

1. S. Guha, C.C. Frazier, P.L. Porter, K. Kang, S. Finberg: Optics Lett. **14**, 952 (1989)
2. P.L. Porter, S. Guha, K. Kang, C.C. Frazier: Polymer (1991) to be published
3. E.W. VanStryland, H. Vanherzeele, M.A. Woodall, M.J. Soileau, A.L. Smirl, S. Guha, T.F. Boggess: Optical Engineering **24**, 613 (1985)
4. J.P. Gordon, R.C.C. Leite, R.S. Moore, S.P.S. Porto, J.R. Whinnery: J. Appl. Phys. **36, 3** (1965)
5. H.S. Carshaw, J.C. Jaeger: *Conduction of Heat in Solids* (Oxford, New York 1959)
6. J.W. Goodman: *Introduction to Fourier Optics* (McGraw-Hill, San Francisco 1968)
7. M. Abramowitz, I.A. Stegun (eds.): *Handbook of Mathematical Functions* (National Bureau of Standards, Washington, DC 1964)